BIOCHEMISTRY
including biophysical chemistry & molecular biology

Article

pubs.acs.org/biochemistry

A Strongly Bound High-Spin Iron(II) Coordinates Cysteine and Homocysteine in Cysteine Dioxygenase

Egor P. Tchesnokov,[†] Sigurd M. Wilbanks,[‡] and Guy N. L. Jameson*,[†]

[†]Department of Chemistry & MacDiarmid Institute for Advanced Materials and Nanotechnology and [‡]Department of Biochemistry, University of Otago, PO Box 56, Dunedin 9054, New Zealand

Supporting Information

ABSTRACT: The first experimental evidence of a tight binding iron(II)−CDO complex is presented. These data enabled the relationship between iron bound and activity to be explicitly proven. Cysteine dioxygenase (CDO) from *Rattus norvegicus* has been expressed and purified with ∼0.17 Fe/polypeptide chain. Following addition of exogenous iron, iron determination using the ferrozine assay supported a very tight stoichiometric binding of iron with an extremely slow rate of dissociation, $k_{off} \sim 1.7 \times 10^{-6}$ s^{-1}. Dioxygenase activity was directly proportional to the concentration of iron. A rate of cysteine binding to iron(III)−CDO was also measured. Mössbauer spectra show that in its resting state CDO binds the iron as high-spin iron(II). This iron(II) active site binds cysteine with a dissociation constant of ∼10 mM but is also able to bind homocysteine, which has previously been shown to inhibit the enzyme.

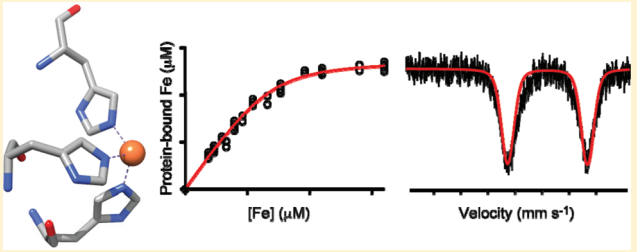

Cysteine dioxygenase[1] (CDO) (EC 1.13.11.20) catalyzes the oxidation of cysteine to cysteine sulfinate[1] through the addition of molecular oxygen to the thiol sulfur (Scheme 1). This is a reaction that has great biological importance as cysteine levels must be tightly controlled *in vivo*, and a breakdown in this control has been linked to many different diseases,[2−4] in part due to interactions with the *N*-methyl-D-aspartate glutamate receptor.[5]

Scheme 1. Reaction Catalyzed by Cysteine Dioxygnease

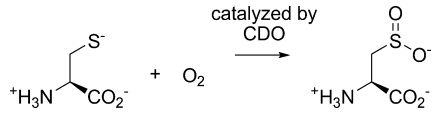

CDO is a non-heme monoiron enzyme belonging to the cupin superfamily defined by the presence of highly conserved motifs $G(X)_5\mathbf{H}X\mathbf{H}(X)_{3,4}\mathbf{E}(X)_6G$ and $G(X)_5PXG(X)_2\mathbf{H}(X)_3N$ (cupin motifs 1 and 2, respectively). The three histidines (H) and one glutamate (E) (highlighted in the text in boldface) are involved in binding a transition metal cofactor required for catalysis. CDO, however, lacks the highly conserved glutamate in cupin motif 1 and uses only the three histidines to bind its ferrous iron cofactor, an aberration from the typical cupin motifs only known to be shared with the diketone-cleaving dioxygenase, Dke1.[6−8]

CDO poses some interesting questions, highlighted by comparisons with other ferrous non-heme monoiron enzymes. Generally, these enzymes can be split into two groups: those that activate the substrate (e.g., homoprotochatechuate-2,3-dioxygenase[9]) and react via an iron(III) superoxo intermediate and those that activate the iron to form high valent iron(IV)oxo intermediates (e.g., taurine dioxygenase (TauD)[10]). It is not yet clear to which group CDO belongs although computational investigations[11,12] predict it reacts via iron(IV)oxo. Previous studies have attempted to answer this question experimentally using crystallography and spectroscopy and following several different approaches.

CDO from mouse,[13] rat,[14,15] and human[16] have all been purified, and crystal structures[13,14,16] are available (Figure 1). It has not yet been possible to crystallize the cysteine-bound form of rat CDO, although this has been achieved with the human form,[16] which has high sequence homology, via cocrystallization. This structure showed that cysteine bound to the iron in a bidentate fashion via the thiol and amine, while the carboxyl group was held in place by R60. These data were at odds with XAS data[17] that suggested the thiol was not bound in the resting state. However, the crystal structure explained the high degree of substrate specifity CDO exhibits and may further explain the ability of homocysteine (hcys) to act as a competitive inhibitor;[1] however, attempts to crystallize CDO in the presence of homocysteine were unsuccessful.[16] When preformed rat CDO crystals were soaked in a cysteine solution, it resulted in an unusual persulfenate[18] complex. It is not yet proven whether this complex is a true intermediate, but it has been investigated computationally[11] and concluded that this constitutes a higher energy pathway and therefore may not be catalytically competent.

Received: October 18, 2011
Revised: November 22, 2011
Published: November 28, 2011

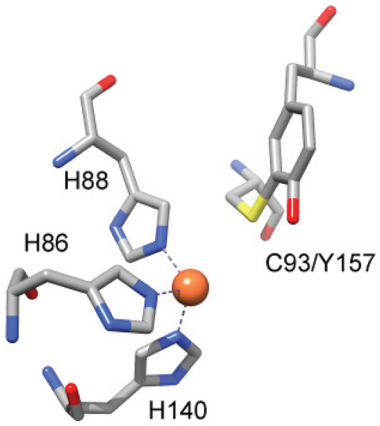

Figure 1. The active site of rat cysteine dioxygenase, showing the coordination of the iron atom by three histidine residues and the cysteine−tyrosine cross-link (PDB 2B5H).

The sequences of mouse and rat are identical and show an intriguing post-translational cross-link[19] between C93 and Y157. This cross-link has been fully characterized by mass spectrometry[20] and shown to be formed in the presence of iron, dioxygen, and high levels of substrate cysteine, particularly at higher pHs. The presence of this cross-link significantly increases activity,[21] although it is not yet known how. It may structurally stabilize an active conformation, and indeed only the cross-linked form appears to crystallize, suggesting it may be less heterogeneous. However, the cross-linked tyrosine residue may act as a proton donor or have a redox role as it does in galactose oxidase.[22] Although not directly coordinated to the iron atom, the tyrosine hydroxyl's close proximity may mean the cross-link also affects iron binding.

Gardner et al. have shown[23] that the UV−vis spectrum of mouse CDO has no distinguishing features. A slight yellow color caused by an increase at 380 nm is present in as-purified protein due to the presence of ∼15% iron(III). This absorption at 380 nm disappeared upon the addition of dithionite. Any iron(III) bound CDO causes a strong blue color to form with an absorption at 640 nm, but no change in absorption is observed upon addition of cysteine when the protein is fully reduced. In contrast, the MCD spectrum of fully reduced CDO shows reasonably intense temperature-dependent features in the near-UV region (<330 nm), which disappear upon exposure to air. This means that, like other non-heme iron(II) enzymes, CDO is not very amenable to study by UV spectroscopy, and more selective techniques are required such as EPR and Mössbauer spectroscopy. The nitrosyl−CDO complex has been studied by EPR spectroscopy,[24] showing that the high-spin iron(II) binds NO after cysteine binding to form a surprisingly low-spin (S = 1/2) $\{FeNO\}^7$ species. This ordered binding is consistent with the well-established NO and O_2 binding behavior exhibited by other iron(II) non-heme monoiron enzymes.[25,26]

Mössbauer spectroscopy[27] has been used extensively to investigate a wide range of enzymes. It is an ideal tool for studying iron containing proteins, and for this reason we have applied the technique to CDO. Specific for ^{57}Fe, the sensitivity of the Mössbauer signal to iron coordination makes Mössbauer spectroscopy particularly useful when studying the interaction of both substrates and inhibitors with the iron center. Mössbauer spectroscopy not only provides direct evidence for interactions but also reports the oxidation state and spin state of the iron atom. This information is provided via experimentally determined parameters: the isomer shift and the quadrupole splitting.

In this study we investigate iron binding to the 3His active site of CDO and deteremine any influence of the cross-link. We also study substrate and inhibitor binding to the iron through Mössbauer spectroscopy and relate this to activity.

EXPERIMENTAL PROCEDURES

Protein Purification. The rat cysteine dioxygenase (rCDO) coding sequence was kindly provided by Dr. Martha H. Stipanuk (Cornell University).[28] The experimental design for the PCR amplification of the rCDO coding sequence was optimized using Primer D'Signer software (IBA). DNA sequence coding for rCDO was PCR-amplified using *Pfu* DNA polymerase (Stratagene) and inserted into pPR-IBA1 expression plasmid (IBA) digested with *Bsa*I (Fermentas), according to standard procedures. CDO was induced in BL21(DE3)pLysS cells (Novagen) and purified using Strep-tag affinity chromatography according to the manufacturer's protocol (IBA).[29,30] We employed the following modifications to the standard protein expression/purification procedures: (i) cells were incubated overnight at 18 °C during protein expression, (ii) cell lysis buffer contained 5 mM divalent ion chelator DTPA (2-[bis[2-[bis(carboxymethyl)amino]ethyl]-amino]acetic acid) in addition to 1 mM EDTA (2,2′,2″,2‴-(ethane-1,2-diyldinitrilo)tetraacetic acid), and (iii) cells were lysed using a French pressure cell press (model FA-078, SLM Aminco). C-terminal Strep-tag affinity technology has been shown to have no effect on the biophysical properties of a homologous dioxygenase[31] and has proven to be a valuable tool in biochemical and structural studies of enzymes.[32,33] The purified protein preparations were dialyzed extensively (>10^9 dilution factor) against buffer containing 40 mM Tris-HCl (pH 8.0) and 50 mM NaCl. Protein was concentrated on Vivaspin centrifugation concentrators (GE Healthscience) to the appropriate concentrations for the subsequent expreiments. Protein concentrations were determined spectrophotometrically at 280 nm using an extinction coefficient of 38 100 M^{-1} cm^{-1}. Consistent with previous observations,[19,20,34] rCDO preparations resolved into two bands when subjected to SDS-PAGE revealing the fraction of the protein with Cys93/Tyr157 cross-link as a result of a post-translational modification (Figure S1). The proportion of the protein with the cross-link was higher than previously reported[20,35] (60%).

Protein preparations were found to be at least 95% pure (Figure S1) and contained ∼20% endogenously bound iron as judged by colorimetric assay using ferrozine.[36] Protein preparations, corresponding buffers and solvents, were made anaerobic by alternating cycles of vacuum and purging with Ar on a Schlenk line kept on ice slurry. All anaerobic manipulations were performed in a glovebox (Belle Technology).

Determination of the Molar Extinction Coefficient. Purified recombinant WT rCDO was centrifuged (4 °C, 20000*g*, 10 min) to remove colloidal matter and any precipitated protein. The UV−vis spectrum of the protein was recorded from 200 to 800 nm, and the absorbance at 280 nm was determined. Aliquots of protein were reduced to dryness using a vacuum centrifuge (SC110 Speed Vac, Savant Instruments). Acid hydrolysis and quantitative amino acid analysis was carried out at Massey University Institute of Food, Nutrition and Human Health,Palmerston North, New Zealand.

The yields of 14 stable amino acids (Asp, Asn, Thr, Pro, Gly, Ala, Val, Ile, Leu, Tyr, Phe, His, Lys, and Arg) were each used to calculate the amount of CDO in the analysis, taking account of the multiplicity of each in CDO. The mean amount of CDO was divided by the volume of the aliquot submitted for amino acid analysis to determine the protein concentration. The ratio of absorbance at 280 nm over the protein concentration determined the rCDO extinction coefficient, ε_{280} = 38 100 M^{-1} cm^{-1}.

Ferrozine Assay. The determination of iron content of protein preparations was adapted from previously described protocols.[7,24,37] We used a colorimetric assay with ferrozine reagent, which forms a stable oxidation-resistant magenta complex with ferrous iron (ε_{562} = 27 900 M^{-1} cm^{-1}).[36,38,39] A 10 μL aliquot of protein preparation was acid-hydrolyzed by addition of 5 μL of concentrated sulfuric acid followed by a 30 min incubation at 95 °C. The sample was briefly spun down and supplemented with 140 μL of ferrozine assay mix resulting in final concentrations of 5 mM ferrozine, 2.6% w/v ascorbic acid, and 387 mM ammonium acetate (pH 9.0). 120 μL was transferred into a 96-well plate, and absorbance at 562 and 750 nm was measured. Absorbance at 750 nm was used as a baseline for all the samples. Absorbance at 562 nm of the buffer corresponding to the protein preparation was treated as a background. A series of iron (ferrous ammonium sulfate) concentrations were assayed in the same manner to generate a standard curve from which a factor correlating absorption at 562 nm to iron concentration in the sample was determined. This procedure allows the determination of total iron concentration in the protein sample. A similar procedure was employed to monitor the release of protein-bound iron into the solvent. For this purpose acid hydrolysis was omitted, and ferrozine assay mix contained ferrozine in 40 mM Tris buffer (pH 8.0) only. No release of protein-bound iron could be detected on an hour time scale (discussed further below). Control experiments confirmed that formation of ferrous iron/ferrozine complex occurs on a substantially faster time scale than ferrous iron oxidation in Tris buffer. A standard experimental setup involved each sample preparation in triplicate.

Iron Dissociation. A stopped-flow apparatus was used to rapidly mix solutions to final concentrations of 15 μM protein active site iron and 6 mM ferrozine. The release of protein-bound iron into the solvent was monitored by measuring over a period of 6 h the formation of a stable oxidation-resistant magenta complex with ferrous iron (ε_{562} = 27 900 M^{-1} cm^{-1}).[36,38,39] The data points were fit using Prism 5 software (GraphPad) to a single-exponential function constrained to a 15 μM amplitude. The resulting fit generated the iron dissociation rate constant of 1.7 × 10^{-6} s^{-1}. Such a slow dissociation rate constant reflects an unusual stability of the protein/iron complex, thereby precluding an accurate determination of the protein/iron dissociation constant.

Iron Binding. The ~70 μM deoxygenated protein samples were mixed anaerobically with eight 1.5-fold increasing concentrations of ferrous sulfate. The resulting concentration range of added ferrous iron was between 9 and 150 μM final. The unbound iron was removed by treating samples with Analytical grade Chelex 100 sodium form, 200−400 mesh (Bio-Rad). Concentrations of protein-bound iron were measured in a ferrozine assay and ploted against the corresponding values of ferrous iron added, which were adjusted for the endogenous iron present in protein preparation after purification. Iron binding by rCDO exhibited a tight binding characteristic, and data points were fit using Prism 5 software (GraphPad) to the following equation:[40] $y = 0.5(K_{app} + E + x) - (0.25(K_{app} + E + x)^2 - Ex)^{1/2}$, where x is the concentration of added iron, y is the concentration of detected protein-bound iron, E is the concentration of protein competent for iron binding, and K_{app} is the apparent dissociation constant for the protein−iron complex as discussed in the Iron Dissociation section. Under our experimental conditions K_{app} approximates the affinity of iron binding to the protein by defining the upper limit for the protein/iron dissociation constant.

Oxygen Electrode. Protein samples generated in iron-binding experiments were mixed with cysteine solution (40 mM Tris, pH 8.0, 50 mM NaCl) to give a final concentration of 10 mM cysteine. The experimental setup involved monitoring the activity of ~70 μM rCDO samples as a function of increasing protein-bound iron concentrations. Dioxygen concentrations were measured on a Clarke-type oxygen electrode (Rank Brothers) with a maximum 1 mL volume. The analogue voltage output was converted to digital readout using a LabTrax AD convertor and stored and analyzed on a PC. Temperature was maintained at 25 °C using a Haake model DC10-K10 refrigerated water circulator thermostat. The reported temperature was found to be optimal for measuring rCDO activity using the oxygen electrode. The electrode was calibrated using Milli-Q water under air-saturated and argon-saturated conditions. 100% air-saturated Milli-Q water was assumed to contain 240 μM dioxygen. The initial velocities of dioxygen depletion in the sample were calculated by conducting a linear regression analysis of the linear portions of polarograms using Prism 5 software (GraphPad).

Stopped Flow. Anaerobic preparation of protein containing 50 μM endogenous iron (17% active sites) was left as is, sample A, or anaerobically iron-saturated by exogenously adding ferrous ammonium sulfate and treating the sample with Analytical grade Chelex 100 sodium form, 200−400 mesh (Bio-Rad), sample B. Sample A was mixed anaerobically with a solution of dithionite to a final concentration of 0.6 mM. Both samples were mixed with equal volumes of anaerobically prepared 20 mM cysteine solution on a stopped-flow apparatus, SX-20MV stopped-flow spectrometer with a Xe-arc lamp (Applied Photophysics). Prior to the experiment the drive syringes and flow circuits were washed with 1 mM dithionite solution and rinsed extensively with deoxygenated buffer. One gram of dithionite was added to the water reservoir of the water circulator. Kinetic experiments were completed in single mixing mode and followed using a photodiode array. Temperature was maintained at 25 °C using a Haake model DC10-K10 refrigerated water circulator thermostat. Single wavelength kinetic traces (380 and 640 nm) were fitted with the SX20 Pro-Data Viewer software (Applied Photophysics). Spectral changes in the region 380−500 nm were analyzed using PC Pro-K global analysis and data simulation software (Applied Photophysics). Further analysis and presentation were completed using Excel (Microsoft) and Prism 5 (GraphPad).

Mössbauer Spectroscopy. Ferrous iron stock solution for Mössbauer spectroscopy experiments was prepared as previously described.[41] Anaerobic preparations of protein (600−750 μM) with ~17% bound iron after purification were iron-saturated anaerobically by exogenously adding ferrous ^{57}Fe (95.4% enriched, SEE Co.) and treating the sample with Analytical grade Chelex 100 sodium form, 200−400 mesh (Bio-Rad). Protein samples were centrifuged at

20000*g* for 30 min at +4 °C, and supernatants were frozen on liquid nitrogen in a glovebox (Belle Technology). Cysteine and homocysteine containing samples had 10 mM final concentrations. Ferrozine-containing samples had 6 mM ferrozine final concentration and were not subject to treatment with Chelex. ^{57}Fe Mössbauer spectra of frozen liquid samples in a custom Teflon sample holder (~400 μL volume) were recorded on a Mössbauer spectrometer from SEE Co. (Science Engineering & Education Co., MN) equipped with a closed-cycle refrigerator system from Janis Research Co. and SHI (Sumitomo Heavy Industries Ltd.) and a temperature controller from Lakeshore Cryotronics, Inc. Data were collected in constant acceleration mode in transmission geometry with an applied field of 47 mT parallel to the γ-rays. The zero velocity of the Mössbauer spectra refers to the centroid of the room temperature spectrum of a 25 μm metallic iron foil. Analysis of the spectra was conducted using the WMOSS program (SEE Co., formerly WEB Research Co., Edina, MN).

RESULTS

Iron Dissociation. Measurement of the dissociation constant for the protein/ligand complex is dependent on the establishment of protein−ligand equilibrium[40] on a time scale compatible with the experimental conditions employed. The current literature[6,37,42] on dioxygenases contains examples of iron dissociation rate constants, k_{off}, ranging from 6×10^{-4} to 4×10^{-5} s^{-1}. This implies that the lower limit for the establishment of protein−ligand equilibrium ranges from half an hour up to 7 h. We used a stopped-flow experiment to determine the iron dissociation rate constant from a 15 μM CDO/iron complex. After 6 h only 0.09% of the 15 μM CDO/iron complex dissociated. Fitting the data to a single-exponential function with the maximum amplitude constrained to a value of 15 μM estimated the iron dissociation constant as 1.7×10^{-6} s^{-1} (Figure S2). Such a slow dissociation rate constant reflects the extreme stability of the CDO/iron complex, which makes impractical an accurate determination of the protein/iron dissociation constant. Therefore, we refer to the CDO/iron dissociation constant determined in the experiments below as an apparent dissociation constant, thus stressing its value as the upper limit.

Iron Binding. A plot of protein-bound iron versus iron added is presented in Figure 2. The data show clearly that iron binding is tight and can be fitted with a single apparent dissociation constant of 5.8 ± 0.6 μM. All data points from three separate experiments are provided to show the spread of the data. The derived estimate for CDO affinity for iron can be compared favorably[7] with the only other enzyme with 3His coordination, Dke1, which has a K_d = 5 μM but also possesses a second weaker binding site with a K_d ~ 3 mM.

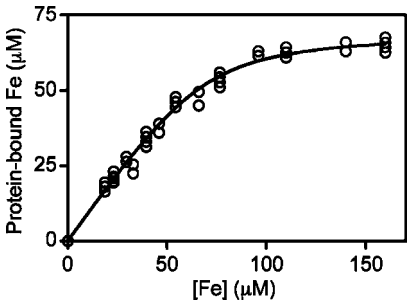

Figure 2. Iron binding by CDO. 70 μM protein was mixed anaerobically with varying concentrations of ferrous sulfate. Unbound iron was removed by Chelex, and the concentration of bound iron was measured using the ferrozine assay. The protein-bound iron is plotted vs the total iron added and fitted according to Experimental Procedures.

CDO Activity. Cysteine dioxygenase activity of protein with different concentrations of iron bound was measured using 10 mM cysteine at pH = 8.0 by following O_2 uptake. [O_2] as a function of time was measured using a Clark-type oxygen electrode and is plotted in Figure 3A. The initial velocites obtained depend linearly on the amount of iron bound (Figure 3B). The slope of the best-fit line is 0.080 s^{-1}.

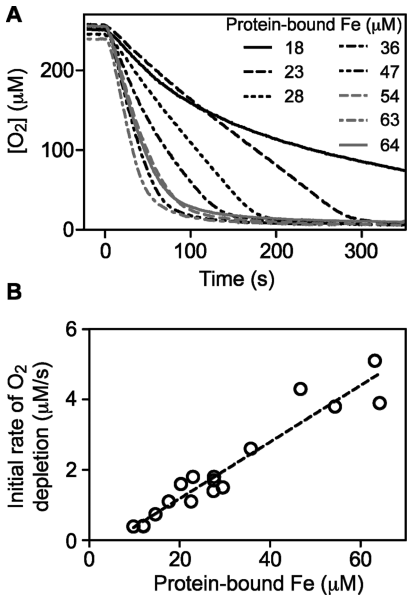

Figure 3. CDO activity. Aliquots of 70 μM CDO with varying amounts of iron bound were reacted with 10 mM cysteine at 25 °C and O_2 uptake measured by oxygen electrode. (A) [O_2] vs time (s). (B) The initial velocities were calculated by linear regession and plotted vs the concentration of protein bound iron. The best-fit line is plotted as a dashed line with a slope of 0.080 s^{-1}.

Stopped Flow of Cysteine Binding. Purified protein contains ~0.17 Fe/protein that is not removed by EDTA and DTPA during purification. Protein was anaerobically iron saturated (as described in Experimental Procedures), and then cysteine binding was measured using stopped flow. Absorption at 380 nm was seen to decrease with concomitant formation of absorption at 640 nm (ε = 630 M^{-1} cm^{-1}) and a clear isosbestic point at 475 nm (Figure 4). These data are consistent with the data published by Gardner et al.[23] and can be explained as binding of cysteine to the endogenous iron(III) form of CDO. This first-order reaction was fitted globally over all wavelengths, and a rate constant of 2.8 s^{-1} was extracted, implying a second-order rate constant for the binding of cysteine to iron(III)CDO of 280 M^{-1} s^{-1}. Prior addition of dithionite abolished any increase in the absorption spectrum (Figure S3), showing that iron(II) binding could not be followed using UV−vis spectroscopy.

Mössbauer Spectroscopy. Mössbauer spectroscopy was used to follow cysteine binding to CDO. Protein preparation was anaerobically ^{57}Fe-saturated as described in Experimental

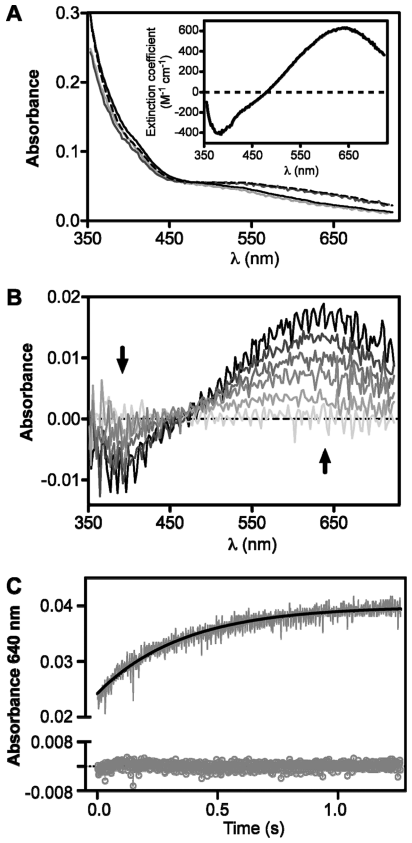

Figure 4. Stopped-flow experiment of cysteine binding to CDO. (A) Absorption spectrum of CDO reacted with cysteine after 1.26 ms and after 1.26 s. Overlaid are the fitted spectra for those times using global analysis. The inset shows the fitted extinction coefficients over all wavelengths showing clearly the presence of two species. (B) Difference spectra taken at 2.5 ms, 40 ms, 0.14 s, 0.25 s, 0.51 s, and 1.26 s, showing the formation of a species absorbing at 640 nm and the disappearance of a band at 380 nm. (C) Increase in absorption at 640 nm versus time. The solid line represents the best-fit line for a single exponential with a rate constant of 2.8 s^{-1}. The residuals are presented below.

Procedures. The spectrum consists of a single broad quadrupole doublet with parameters (δ = 1.22 mm s^{-1}; ΔE_Q = 2.76 mm s^{-1}; $\Gamma_{L=R}$ = 0.55 mm s^{-1} (Voigt line shape)) consistent with high-spin iron(II). The parameters are, however, remarkably similar to iron(II) in solution. To check that this was the spectrum of iron bound CDO, protein was allowed to react with ^{57}Fe and then mixed with a solution containing in excess of 3 mol equiv of the strong iron chelator ferrozine to ensure that all iron was bound. The spectrum (Figure S4) consists of two overlapping quadrupole doublets with one representative of $[Fe(ferrozine)_3]^{4-}$. When a reference spectrum of the ferrozine complex is subtracted from this spectrum, a quadrupole doublet remains that is identical to the spectrum of iron(II) bound CDO above. This provides the evidence for a tightly bound iron(II) within the active site of CDO. Addition of excess ferrozine did not produce a single quadrupole doublet consistent with low-spin iron(II), showing that CDO active site iron(II) is not subject to chelation by ferrozine. Considering that the stability constant[43] of $[Fe(ferrozine)_3]^{4-}$ is log β_3 = 15.86, this result was suprising. This observation is, however, in line with our iron binding experiments showing a tight binding characteristic for the iron(II)−CDO complex. Iron(III) bound protein can be reduced by dithionite, and the spectrum is very similar but has a slightly larger quadrupole splitting (Figure 5). This is most likely a pH effect since it has been previously observed that the quadrupole splitting increases with decreasing pH in frozen protein solutions.[44]

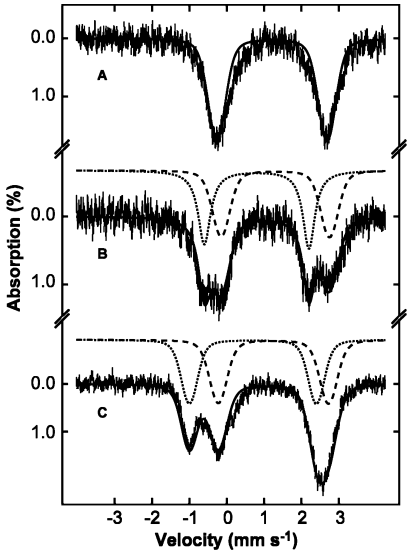

Figure 5. Mössbauer spectra of CDO. (A) 0.73 mM CDO with 0.56 mM $^{57}Fe^{2+}$ bound. (B) Sample A mixed anaerobically with 10 mM final cysteine. The spectrum can be fitted to two quadrupole doublets representing bound (dotted line) and unbound (dashed line). (C) 0.62 mM CDO mixed with 10 mM homocysteine. Again, the spectrum can be fitted to two quadrupole doublets similar to those for cysteine above. All parameters are given in Table 1.

Anaerobic addition of 10 mM cysteine causes a dramatic change in the spectrum (Figure 5). A new quadrupole doublet appears that has a lower isomer shift and quadrupole splitting. Similar results are found regardless of whether dithionite is present (Figure S5). The lower isomer shift (Table 1) could indicate a decrease in the coordination number with the replacement of three waters by the cysteine as suggested by the crystal structure. It does show that iron(II) CDO can bind cysteine without electron transfer from iron to the thiol to form a thiyl radical.

Addition of homocysteine produces a similar change in the Mössbauer spectrum, and the paramaters are remarkably similar, indicating a binding mode comparable to that of cysteine. Homocysteine has previously been reported to inhibit CDO activity through binding to the active site.[15,17]

DISCUSSION

Cysteine dioxygenase has unusual coordination around the iron atom. The 3His motif appears to be rare compared with the more usual 2His1Asp/Glu binding that is prevalent in non-heme monoiron(II) enzymes. It has been suggested[45] that this coordination is essential for optimal dioxygenation of the substrate. In this paper we show that this neutral ligand set is a strong binder of iron(II). To our knowledge, this is the first experimental evidence to suggest a tight-binding iron(II)−CDO complex. The data presented clearly show that a maximum of one iron is bound per protein with CDO that is 60% cross-linked. It therefore appears that iron binding is independent of whether the cross-link is present. This view is supported by a tight iron(II)−CDO complex exhibiting similar

dx.doi.org/10.1021/bi201597w | *Biochemistry* 2012, 51, 257−264

Table 1. Mössbauer Parameters of Cysteine Dioxygenase Measured at 5.2 K

		δ (mm s^{-1})	ΔE_Q (mm s^{-1})	Γ_L (mm s^{-1})[a]	Γ_R (mm s^{-1})	I (%)
Fe(II)-CDO		1.22	2.76	0.55	0.55	100
Fe(II)-CDO (dithionite reduced)		1.21	2.95	0.55	0.55	100
Fe(II)-CDO-cys	unbound	1.30	2.90	0.55	0.55	50
	bound	0.80	2.80	0.40	0.38	50
Fe(II)-CDO-hcys	unbound	1.25	2.95	0.55	0.55	50
	bound	0.70	3.40	0.50	0.50	50

[a]All spectra were fitted using a Voigt line shape.

affinity for iron(II) as Dke1 (dissociation constant = 5 μM) that coordinates iron(II) but does not possess a Cys-Tyr cross-link.[31]

O_2 electrode data show that the iron is necessary for activity, and the rate is proportional to the amount of iron bound, further supporting strong iron binding. To our knowledge, this is the first experimental evidence directly correlating the iron-based active site concentration with the rate of oxygen substrate usage by CDO. In previous work a large excess of iron was needed to gain maximum activity.[34] The rate of 0.080 s^{-1} corresponds to 4.8 oxygen substrate turnovers per minute conducted by CDO at 25 °C and pH 8 and cannot be directly compared with previously reported values due to the different experimental conditions but is of a similar order of magnitude.

Iron(III)−CDO, present in small amounts unless reduced by dithionite, binds cysteine to form a blue absorption centered around 640 nm with an extinction coefficient the same as previously[23] published. It forms with a rate constant of 2.8 s^{-1}, which corresponds to a second-order rate constant of 280 M^{-1} s^{-1}. This is an order of magnitude slower than 2,4-pentanedione binding to Dke1.[31] Unfortunately, cysteine binding to iron(II)−CDO elicits no color change, but a comparable rate of binding can be expected.

Mössbauer spectra have been obtained of CDO enriched with ^{57}Fe, and they exhibit a single quadrupole doublet. The combination of it being a wide quadrupole doublet (ΔE_Q = 2.8 mm s^{-1}) and the isomer shift (δ = 1.2 mm s^{-1}) is very distinctive. These results show that the iron is integer spin (S = 2) iron(II) with O and N coordination and in fact has parameters similar to iron(II) in solution in Tris buffer. The quadrupole doublets have Voigt line shape, indicating a certain amount of heterogeneity in the active site, but this is not unusual.[10,46] In fact, these parameters are comparable with other non-heme monoiron enzymes such as protocatechuate 4,5 dioxygenase[46] and isopenicillin N synthase.[47] This similarity is striking because CDO has iron bound by three histidines rather than by 2His1carboxylate, like the other enzymes mentioned, and this difference may have been expected to change the quadrupole splitting through changes in covalency.

Addition of cysteine results in the emergence of a new quadrupole doublet with parameters also consistent with high-spin iron(II). The isomer shift decreases considerably (by 0.4 mm s^{-1}), suggesting a more covalent iron ligand environment and a lowering of the coordination number as cysteine binds in a bidentate fashion, replacing three water molecules. The active site is now primed for addition of dioxygen and further reaction. Such changes, although not as dramatic as presented here, have been observed previously in the Mössbauer spectrum of other monoiron enzymes[46,47] upon substrate binding. These changes in coordination have also been followed by resonance Raman spectroscopy.[48]

Scheme 2. Reaction of Cysteine and Homocysteine with CDO

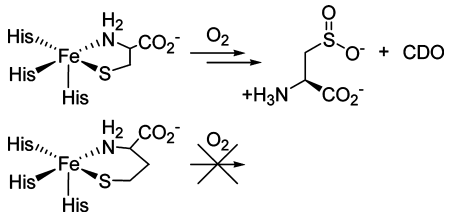

The cysteine-bound species produces a doublet that constitutes 50% of the total area. Using a ^{57}Fe concentration of 0.52 mM, this corresponds to a K_d of ∼10 mM, which is similar to substrate binding by isopenicillin N synthase.[47] This value of K_d also correlates well with the Michaelis−Menten constant for cysteine measured by us[49] and others, suggesting k_{-1} must be greater than k_2. Furthermore, if the rate of cysteine binding to iron(II)−CDO is approximated to that of cysteine binding to iron(III)−CDO given above, then using K_d, k_{-1} = 3 s^{-1}, and this is indeed greater than k_2 given by our oxygen electrode data (0.080 s^{-1}). Taken all together, the data provide a robust description of CDO reaction kinetics.

Addition of racemic homocysteine results in a very similar Mössbauer spectrum, and this is consistent with a very similar mode of binding. However, homocysteine is not oxidized, and therefore there must be an energetic reason why formation of the iron(II)CDO−homocysteine complex either does not bind dioxygen or does not activate it ready for reaction. This is likely to be because homocysteine allows the formation of a more stable 6-membered chelate (Scheme 2). This raises further important questions about substrate specifity. It is not yet clear what differences make CDO so cysteine specific, especially when certain bacteria[50] possess enzymes capable of carrying out the same oxidation of the related molecule 3-mercaptopropionic acid.

In conclusion, CDO tightly binds iron(II) at a 3His active site. Although the cross-link between C93 and Y157 is close to the active site, it does not appear to affect iron binding because the results presented here are similar to the enzyme Dke1, which has a 3His active site but does not possess a cross-link. Iron dissociation from the CDO active site exhibits an extremely slow dissociation rate constant, illustrating the stability of the resting state CDO. Mössbauer spectroscopy shows that this iron(II) site can bind either cysteine or homocysteine, leading to a change of coordination that prepares the enzyme for O_2 addition.

dx.doi.org/10.1021/bi201597w | Biochemistry 2012, 51, 257−264

■ ASSOCIATED CONTENT

Supporting Information

SDS-PAGE to show protein purity, stopped-flow data, and Mössbauer spectra. This material is available free of charge via the Internet at http://pubs.acs.org.

■ AUTHOR INFORMATION

Corresponding Author

*Tel: +64 3 479 8028. Fax: +64 3 479 7906. E-mail: gjameson@chemistry.otago.ac.nz.

Funding

This work was supported by the Marsden fund of the Royal Society of New Zealand (grant UOO0923).

■ ACKNOWLEDGMENTS

The authors thank Lottery Health Research (New Zealand).

■ REFERENCES

(1) Joseph, C. A., and Maroney, M. J. (2007) Cysteine dioxygenase: structure and mechanism. *Chem. Commun.*, 3338−3349.

(2) Jameson, G. N. L. (2011) Iron, cysteine and Parkinson's disease. *Monatsh. Chem. 142*, 325−329.

(3) Jameson, G. N. L., Zhang, J., Jameson, R. F., and Linert, W. (2004) Kinetic evidence that cysteine reacts with dopaminoquinone via reversible adduct formation to yield 5-cysteinyl-dopamine: an important precursor of neuromelanin. *Org. Biomol. Chem. 2*, 777−782.

(4) Ueki, I., Roman, H. B., Valli, A., Fieselmann, K., Lam, J., Peters, R., Hirschberger, L. L., and Stipanuk, M. H. (2011) Knockout of the cysteine dioxygenase gene results in severe impairment in taurine synthesis and increased catabolism of cysteine to hydrogen sulfide. *Am. J. Physiol. Endocrinol. Metab. 301*, E668−E684.

(5) Olney, J. W., Zorumski, C., Price, M. T., and Labruyere, J. (1990) L-cysteine, a bicarbonate-sensitive endogenous excitotoxin. *Science 248*, 596.

(6) Diebold, A. R., Neidig, M. L., Moran, G. R., Straganz, G. D., and Solomon, E. I. (2010) The Three-His Triad in Dke1: Comparisons to the Classical Facial Triad. *Biochemistry 49*, 6945−6952.

(7) Leitgeb, S., Straganz, G. D., and Nidetzky, B. (2009) Biochemical characterization and mutational analysis of the mononuclear non-haem Fe^{2+} site in Dke1, a cupin-type dioxygenase from *Acinetobacter johnsonii*. *Biochem. J. 418*, 403−411.

(8) Straganz, G. D., Glieder, A., Brecker, L., Ribbons, D. W., and Steiner, W. (2003) Acetylacetone-cleaving enzyme Dke1: a novel C-C-bond-cleaving enzyme from *Acinetobacter johnsonii*. *Biochem. J. 369*, 573−581.

(9) Mbughuni, M. M., Chakrabarti, M., Hayden, J. A., Bominaar, E. L., Hendrich, M. P., Munck, E., and Lipscomb, J. D. (2010) Trapping and spectroscopic characterization of an Fe(III)-superoxo intermediate from a nonheme mononuclear iron-containing enzyme. *Proc. Natl. Acad. Sci. U. S. A. 107*, 16788−16793.

(10) Price, J. C., Barr, E. W., Tirupati, B., Bollinger, J. M. Jr., and Krebs, C. (2003) The first direct characterization of a high-valent iron intermediate in the reaction of an alpha -ketoglutarate-dependent dioxygenase: A high-spin Fe(IV) complex in taurine/alpha -ketoglutarate dioxygenase (TauD) from Escherichia coli. *Biochemistry 42*, 7497−7508.

(11) Kumar, D., Thiel, W., and de Visser, S. P. (2011) Theoretical Study on the Mechanism of the Oxygen Activation Process in Cysteine Dioxygenase Enzymes. *J. Am. Chem. Soc. 133*, 3869−3882.

(12) Aluri, S., and De Visser, S. P. (2007) The Mechanism of Cysteine Oxygenation by Cysteine Dioxygenase Enzymes. *J. Am. Chem. Soc. 129*, 14846−14847.

(13) McCoy, J. G., Bailey, L. J., Bitto, E., Bingman, C. A., Aceti, D. J., Fox, B. G., and Phillips, G. N. Jr. (2006) Structure and mechanism of mouse cysteine dioxygenase. *Proc. Natl. Acad. Sci. U. S. A. 103*, 3084−3089.

(14) Simmons, C. R., Liu, Q., Huang, Q., Hao, Q., Begley, T. P., Karplus, P. A., and Stipanuk, M. H. (2006) Crystal Structure of Mammalian Cysteine Dioxygenase: a novel mononuclear iron center for cysteine thiol oxidation. *J. Biol. Chem. 281*, 18723−18733.

(15) Chai, S. C., Jerkins, A. A., Banik, J. J., Shalev, I., Pinkham, J. L., Uden, P. C., and Maroney, M. J. (2005) Heterologous expression, purification, and characterization of recombinant rat cysteine dioxygenase. *J. Biol. Chem. 280*, 9865−9869.

(16) Ye, S., Wu, X., Wei, L., Tang, D., Sun, P., Bartlam, M., and Rao, Z. (2007) An Insight into the Mechanism of Human Cysteine Dioxygenase. Key Roles of the Thioether-Bonded Tyrosine-Cysteine Cofactor. *J. Biol. Chem. 282*, 3391−3402.

(17) Chai, S. C., Bruyere, J. R., and Maroney, M. J. (2006) Probes of the catalytic site of cysteine dioxygenase. *J. Biol. Chem. 281*, 15774−15779.

(18) Simmons, C. R., Krishnamoorthy, K., Granett, S. L., Schuller, D. J., Dominy, J. E., Begley, T. P., Stipanuk, M. H., and Karplus, P. A. (2008) A Putative Fe^{2+}-Bound Persulfenate Intermediate in Cysteine Dioxygenase. *Biochemistry 47*, 11390−11392.

(19) Dominy, J. E. Jr., Hwang, J., Guo, S., Hirschberger, L. L., Zhang, S., and Stipanuk, M. H. (2008) Synthesis of Amino Acid Cofactor in Cysteine Dioxygenase Is Regulated by Substrate and Represents a Novel Post-translational Regulation of Activity. *J. Biol. Chem. 283*, 12188−12201.

(20) Kleffmann, T., Jongkees, S. A. K., Fairweather, G., Wilbanks, S. M., and Jameson, G. N. L. (2009) Mass-spectrometric characterization of two posttranslational modifications of cysteine dioxygenase. *J. Biol. Inorg. Chem. 14*, 913−921.

(21) Siakkou, E., Rutledge, M. T., Wilbanks, S. M., and Jameson, G. N. L. (2011) Correlating Crosslink Formation with Enzymatic Activity in Cysteine Dioxygenase. *Biochim. Biophys. Acta, Proteins Proteomics 1814*, 2003−2009.

(22) Rogers, M. S., Hurtado-Guerrero, R. n., Firbank, S. J., Halcrow, M. A., Dooley, D. M., Phillips, S. E. V., Knowles, P. F., and McPherson, M. J. (2008) Cross-Link Formation of the Cysteine 228 - Tyrosine 272 Catalytic Cofactor of Galactose Oxidase Does Not Require Dioxygen. *Biochemistry 47*, 10428−10439.

(23) Gardner, J. D., Pierce, B. S., Fox, B. G., and Brunold, T. C. (2010) Spectroscopic and Computational Characterization of Substrate-Bound Mouse Cysteine Dioxygenase: Nature of the Ferrous and Ferric Cysteine Adducts and Mechanistic Implications. *Biochemistry 49*, 6033−6041.

(24) Pierce, B. S., Gardner, J. D., Bailey, L. J., Brunold, T. C., and Fox, B. G. (2007) Characterization of the Nitrosyl Adduct of Substrate-Bound Mouse Cysteine Dioxygenase by Electron Paramagnetic Resonance: Electronic Structure of the Active Site and Mechanistic Implications. *Biochemistry 46*, 8569−8578.

(25) Que, L., and Ho, R. Y. N. (1996) Dioxygen Activation by Enzymes with Mononuclear Non-Heme Iron Active Sites. *Chem. Rev. 96*, 2607−2624.

(26) Costas, M., Mehn, M. P., Jensen, M. P., and Que, L. Jr. (2004) Dioxygen Activation at Mononuclear Nonheme Iron Active Sites: Enzymes, Models, and Intermediates. *Chem. Rev. 104*, 939−986.

(27) Gütlich, P., Bill, E., and Trautwein, A. X. (2011) *Mössbauer Spectroscopy and Transition Metal Chemistry: Fundamentals and Applications*, Springer-Verlag, Berlin.

(28) Simmons, C. R., Hao, Q., and Stipanuk, M. H. (2005) Preparation, crystallization and X-ray diffraction analysis to 1.5 A resolution of rat cysteine dioxygenase, a mononuclear iron enzyme responsible for cysteine thiol oxidation. *Acta Crystallogr., Sect. F: Struct. Biol. Cryst. Commun. 61*, 1013−1016.

(29) Schmidt, T. G. M., and Skerra, A. (2007) The Strep-tag system for one-step purification and high-affinity detection or capturing of proteins. *Nature Protocols 2*, 1528−1535.

(30) Skerra, A., and Schmidt, T. G. (2000) Use of the Strep-Tag and streptavidin for detection and purification of recombinant proteins. *Methods Enzymol. 326*, 271−304.

(31) Straganz, G. D., Diebold, A. R., Egger, S., Nidetzky, B., and Solomon, E. I. (2010) Kinetic and CD/MCD Spectroscopic Studies of

the Atypical, Three-His-Ligated, Non-Heme Fe^{2+} Center in Diketone Dioxygenase: The Role of Hydrophilic Outer Shell Residues in Catalysis. *Biochemistry 49*, 996−1004.
(32) Tchesnokov, E. P., Obikhod, A., Schinazi, R. F., and Gotte, M. (2009) Engineering of a chimeric RB69 DNA polymerase sensitive to drugs targeting the cytomegalovirus enzyme. *J. Biol. Chem. 284*, 26439−26446.
(33) Zahn, K. E., Tchesnokov, E. P., Gotte, M., and Doublie, S. (2011) Phosphonoformic acid inhibits viral replication by trapping the closed form of the DNA polymerase. *J. Biol. Chem.*, in press.
(34) Simmons, C. R., Hirschberger, L. L., Machi, M. S., and Stipanuk, M. H. (2006) Expression, purification, and kinetic characterization of recombinant rat cysteine dioxygenase, a non-heme metalloenzyme necessary for regulation of cellular cysteine levels. *Protein Expression Purif. 47*, 74−81.
(35) Stipanuk, M. H., Hirschberger, L. L., Londono, M. P., Cresenzi, C. L., and Yu, A. F. (2004) The ubiquitin-proteasome system is responsible for cysteine-responsive regulation of cysteine dioxygenase concentration in liver. *Am J. Physiol. Endocrinol. Metab. 286*, E439−448.
(36) Stookey, L. L. (1970) Ferrozine - a new spectrophotometric reagent for iron. *Anal. Chem. 42*, 779−781.
(37) Johnson-Winters, K., Purpero, V. M., Kavana, M., Nelson, T., and Moran, G. R. (2003) (4-Hydroxyphenyl)pyruvate Dioxygenase from Streptomyces avermitilis: The Basis for Ordered Substrate Addition. *Biochemistry 42*, 2072−2080.
(38) Gibbs, C. R. (1976) Characterization and Application of FerroZine Iron Reagent as a Ferrous Iron Indicator. *Anal. Chem. 48*, 1197−1201.
(39) Berlett, B. S., Levine, R. L., Chock, P. B., Chevion, M., and Stadtman, E. R. (2001) Antioxidant activity of Ferrozine-iron-amino acid complexes. *Proc. Natl. Acad. Sci. U. S. A. 98*, 451−456.
(40) Copeland, R. A. (2000) *Enzymes - A Practical Introduction to Structure, Mechanism, and Data Analysis*, 2nd ed., Wiley-VCH, Inc., New York.
(41) Bollinger, J. M., Tong, W. H., Ravi, N., Huynh, B. H., Edmonson, D. E., and Stubbe, J. (1994) Mechanism of Assembly of the Tyrosyl Radical-Diiron(III) Cofactor of E. coli Ribonucleotide Reductase. 2. Kinetics of The Excess Fe2+ Reaction by Optical, EPR, and Moessbauer Spectroscopies. *J. Am. Chem. Soc. 116*, 8015−8023.
(42) Amaya, A. A., Brzezinski, K. T., Farrington, N., and Moran, G. R. (2004) Kinetic analysis of human homogentisate 1,2-dioxygenase. *Arch. Biochem. Biophys. 421*, 135−142.
(43) Thompsen, J. C., and Mottola, H. A. (1984) Kinetics of the complexation of iron(II) with ferrozine. *Anal. Chem. 56*, 755−757.
(44) Horner, O., Mouesca, J. M., Solari, P. L., Orio, M., Oddou, J. L., Bonville, P., and Jouve, H. M. (2007) Spectroscopic description of an unusual protonated ferryl species in the catalase from Proteus mirabilis and density functional theory calculations on related models. Consequences for the ferryl protonation state in catalase, peroxidase and chloroperoxidase. *J. Biol. Inorg. Chem. 12*, 509−525.
(45) de Visser, S. P., and Straganz, G. D. (2009) Why Do Cysteine Dioxygenase Enzymes Contain a 3-His Ligand Motif Rather than a 2His/1Asp Motif Like Most Nonheme Dioxygenases? *J. Phys. Chem. A 113*, 1835−1846.
(46) Arciero, D. M., Lipscomb, J. D., Huynh, B. H., Kent, T. A., and Munck, E. (1983) Electron-Paramagnetic-Res and Mossbauer Studies of Protocatechuate 4,5-Dioxygenase - Characterization of a New Fe-2+ Environment. *J. Biol. Chem. 258*, 14981−14991.
(47) Orville, A. M., Chen, V. J., Kriauciunas, A., Harpel, M. R., Fox, B. G., Munck, E., and Lipscomb, J. D. (1992) Thiolate Ligation of the Active-Site Fe2+ of Isopenicillin-N Synthase Derives from Substrate Rather Than Endogenous Cysteine - Spectroscopic Studies of Site-Specific Cys -] Ser Mutated Enzymes. *Biochemistry 31*, 4602−4612.
(48) Ho, R. Y. N., Mehn, M. P., Hegg, E. L., Liu, A., Ryle, M. J., Hausinger, R. P., and Que, L. Jr. (2001) Resonance Raman studies of the iron(II)-alpha -keto acid chromophore in model and enzyme complexes. *J. Am. Chem. Soc. 123*, 5022−5029.
(49) Siakkou, E., Wilbanks, S. M., and Jameson, G. N. L. (2010) Simplified cysteine dioxygenase activity assay allows simultaneous quantitation of both substrate and product. *Anal. Biochem. 405*, 127−131.
(50) Bruland, N., Wubbeler, J. H., and Steinbuchel, A. (2009) 3-Mercaptopropionate Dioxygenase, a Cysteine Dioxygenase Homologue, Catalyzes the Initial Step of 3-Mercaptopropionate Catabolism in the 3,3-Thiodipropionic Acid-degrading Bacterium Variovorax paradoxus. *J. Biol. Chem. 284*, 660−672.